ON THE NUMERICAL CONVERGENCE TO STEADY STATE OF HYPERSONIC FLOWS OVER BODIES WITH CONCAVITIES

Peter A. Gnoffo
Mail Stop 408A
NASA Langley Research Center
Hampton, VA 23681-0001
p.a.gnoffo@larc.nasa.gov

Abstract. Two recent numerical studies of hypersonic flows over bodies with concavities revealed problems with convergence to a steady state with an oft-used application of local-time-stepping. Both simulated flows showed a time-like, periodic shedding of vortices in a subsonic domain bounded by supersonic external flow although the simulations, using local-time-stepping, were not time accurate. Simple modifications to the numerical algorithm were implemented to enable implicit, first-order accurate in time simulations. Subsequent time-accurate simulations of the two test problems converged to a steady state. The baseline algorithm and modifications for temporal accuracy are described. The requirement for sub-iterations to achieve convergence is demonstrated. Failure to achieve convergence without time accuracy is conjectured to arise from temporal errors being continuously refocused into a subsonic domain.

Key words: unsteady, hypersonic, local-time-stepping, time-accurate, ballute

1 INTRODUCTION

Two recent numerical studies of hypersonic flows over bodies with concavities revealed problems with convergence to a steady state with an oft-used application of local-time-stepping. A concavity is defined as any region over which outward running normals to the surface intersect. Compression corners are included in this definition of concavity.

The first study[1] involved a code validation experiment[2] of Mach 9.5 flow over a sharp, double-cone at Re/m = 264000 (Run 24) in which experimental data indicated steady flow but the numerical simulation failed to converge. In contrast, a numerical simulation of Run 28 over the same configuration at Mach 9.6 but with a lower Reynolds number (Re/m =144000) converged to a steady state for all grids and physical models tested. At the time, it was thought that the non-linear Symmetric Total Variation (STVD)[3] limiter caused the problem because an unlimited, first-order simulation converged (albeit a poor simulation of the experiment.)

The second study involved towed, inflatable, ballute (balloon-parachute) decelerators in which hypersonic flow over concave shapes would not support a steady, external

hypersonic flow[4]. A spherical segment depression with rounded shoulders supported a pulsing wave in which the bow shock oscillated over a distance exceeding the outer radius of the ballute. (The simulation was for a uniform, incoming flow – it did not include the wake of the towing spacecraft.) The existence of an unsteady flow in this case was not surprising; cavities in the stagnation region of blunt bodies are known to induce unsteadiness[5].

Both simulated flows showed a time-like, periodic shedding of vortices in a subsonic domain bounded by supersonic external flow although the simulation, using local-time-stepping, was not time accurate. Simple modifications to the numerical algorithm were implemented to enable implicit, first-order in time simulations. Subsequent time-accurate simulations of the two test problems converged to a steady state. The baseline algorithm and modifications for temporal accuracy are described. The requirement for sub-iterations to achieve convergence is demonstrated. Failure to achieve convergence without time accuracy is conjectured to arise from temporal errors being continuously refocused into a subsonic domain. The failure to converge using local-time-stepping is not evident in all simulations of hypersonic flows over concavities; the dependence on specific details of the algorithm, geometry, and flow parameters require additional study.

All of the numerical simulations discussed herein are executed using the Langley Aerothermodynamic Upwind Relaxation Algorithm (LAURA).[6,7] This paper reviews implicit algorithms as applied in LAURA based on single-level storage local-time-stepping and two-level storage using sub-iterations to achieve first-order time accuracy. These details are reviewed because they strongly influence the evolution of an "unsteady" response in the test cases.

2 ALGORITHM

2.1 Point-Implicit Relaxation

The Langley Aerothermodynamic Upwind Relaxation Algorithm (LAURA) employs two relaxation modes: point-implicit and line-implicit. The point- implicit mode implicitly solves only contributions of dependent variables at cell L, $\overline{q}_L$, to the residual at cell L, $\overline{r}_L$; contributions from dependent variables at neighbor cells are treated explicitly. The contributions of inviscid, viscous, and source terms are included in the point-implicit matrix, B_L, as follows:

$$\mathcal{B}_L = \mathcal{S}_L \Omega_L + c_1 \mathcal{M}_L + c_2 \mathcal{N}_L \tag{1}$$

where S_L is the Jacobian of the chemical and thermal source term components of the residual, M_L is the Jacobian of the inviscid terms, and N_L is the Jacobian of the viscous terms – all with respect to $\overline{q}_L$. Scalar constants c_1>1.5 and c_2>0.5 are relaxation factors. Typical values are c_1=3 and c_2=1. Relaxation factors on the source term Jacobian have never been required.

Within the context of flux difference splitting (FDS) and Roe's averaging[8] the inviscid Jacobian is defined:

$$\mathcal{M}_L = \frac{1}{2} \sum_m |A_m| \, \sigma_m \tag{2}$$

where m is summed over all faces of cell L, A_m is the Roe's averaged flux Jacobian at face m, and $|A_m|$ is defined using the absolute values of the eigenvalues of A_m. The elements of A_m are required in the definition of the FDS formulation of the inviscid flux; consequently, it is economical to reuse these quantities in the formulation of the Jacobian. The absolute value of the eigenvalues may be limited from below using a variation of Harten's entropy fix[9,3].

The viscous Jacobian is defined:

$$\mathcal{N}_L = \sum_m B_m \sigma_m \tag{3}$$

where B_m is the Jacobian of viscous terms across the m^{th} face of cell L. It implicitly treats only the divided difference across the cell face. Transport properties at cell face m are linear averages of adjacent cell center values. Velocities in the shear work term are the Roe averaged quantities already computed for the inviscid flux function. Eigenvalues of B_m are positive or zero.

The change in dependent variables after a single, point-implicit relaxation step is computed as follows:

$$\left[\frac{\Omega_L}{\Delta t_L} I + \mathcal{B}_L\right]\Delta\bar{q}_L = \bar{r}_L \tag{4}$$

where I - the identity matrix, Ω_L - the volume, and Δt_L - the time step at cell L (usually derived from a constant Courant number, local-time-stepping, specification) are associated with the time derivative term of the conservation equations. In the present study, Δt_L is based on Courant numbers of 10^1 and 10^6 as well as constant values for all indices.

2.2 Line-Implicit Relaxation

The point-implicit option is not efficient for relaxing the viscous layers. Some efficiency can be recovered by using multitasking with majority of cycles in the boundary layer or by using an over-relaxation factor $1>c_2>0.5$. However, a better approach is to introduce implicit dependence of the solution across the entire shock layer.

The line-implicit relaxation algorithm is a simple extension of the point-implicit algorithm. However, approximations to A_L, the Jacobian of $\bar{r}_L$ with respect to $\bar{q}_{L-1}$, and C_L, the Jacobian of $\bar{r}_L$ with respect to $\bar{q}_{L+1}$, are introduced to preserve symmetry of form with B_L that also improves convergence. They are defined:

$$\mathcal{a}_L = \left[-\frac{c_1}{2}\left(|A_{L-1/2}| + A_{L-1/2}\right) - c_2 B_{L-1/2}\right]\sigma_{L-1/2} \tag{5a}$$

$$\mathcal{c}_L = \left[-\frac{c_1}{2}\left(|A_{L+1/2}| - A_{L+1/2}\right) - c_2 B_{L+1/2}\right]\sigma_{L+1/2} \tag{5b}$$

It is assumed that sequential indices L define a continuous series of cells spanning some portion of the computational domain. The subscripts $L \pm 1/2$ refer to Roe averaged conditions on face m between cell centers L and $L \pm 1$, respectively. A more exact linearization of the residual would lead to use of $A_{L+/-1}$ in place of $A_{L+/-1/2}$ in the second occurrence of Eqs. 5; however, the present formulation provides exact cancellation of convective, downwind implicit influences and exhibits more robust convergence characteristics, particularly in the vicinity of strong shock waves at large Courant numbers.

In the present work, the source term requires no off-diagonal, implicit contribution. The line-implicit relaxation in Eq. (6) requires approximately 2.8 times more CPU time per iteration as the point-implicit algorithm in the applications described here but convergence rate more than makes up for this overhead. It requires additional storage for the off-diagonal blocks.

$$\begin{bmatrix} \mathcal{B}_L & \mathcal{C}_L & 0 & 0 & 0 \\ \mathcal{A}_{L+1} & \mathcal{B}_{L+1} & \mathcal{C}_{L+1} & 0 & 0 \\ 0 & \ddots & \ddots & \ddots & 0 \\ 0 & 0 & \mathcal{A}_{L+N-1} & \mathcal{B}_{L+N-1} & \mathcal{C}_{L+N-1} \\ 0 & 0 & 0 & \mathcal{A}_{L+N} & \mathcal{B}_{L+N} \end{bmatrix} \begin{bmatrix} \Delta\bar{q}_L \\ \Delta\bar{q}_{L+1} \\ \vdots \\ \Delta\bar{q}_{L+N-1} \\ \Delta\bar{q}_{L+N} \end{bmatrix} = \begin{bmatrix} \bar{r}_L \\ \bar{r}_{L+1} \\ \vdots \\ \bar{r}_{L+N-1} \\ \bar{r}_{L+N} \end{bmatrix} \tag{6}$$

2.3 Implicit Boundary Conditions

Implicit treatment of boundary conditions is required to obtain good convergence with line relaxation. Boundary conditions in the present formulation are implemented with ghost cells. If the off-diagonal Jacobian at the ghost cell for L=1is A_0 then B_1 is augmented by $A_0 \mathcal{W}_0^{-1} \mathcal{W}_1$ where:

$$\mathcal{W}_0 d\bar{q}_0 = \mathcal{W}_1 d\bar{q}_1 \tag{7}$$

is an expression of the dependence of the ghost cell on the boundary cell. In like manner, B_N is augmented by $C_{N+1} \mathcal{W}_{N+1}^{-1} \mathcal{W}_N$ where $\mathcal{W}_{N+1} d\bar{q}_{N+1} = \mathcal{W}_N d\bar{q}_N$.

2.4 Time Accuracy

The LAURA algorithm, in its default mode, uses single level storage and relaxes the steady form of the governing equations with a Courant number of 10^6. However, some applications considered here require time-accurate relaxation. Time accuracy (first-order in Δt) can be recovered by using constant time step advancement at all cells and by employing two levels of storage with sub-iterations to converge the current iterate before advancing to the next time level[10].

$$\left[\frac{\Omega_L}{\Delta t} I + \mathcal{B}_L \right] \Delta\bar{q}_L^{k+1} = \bar{r}_L^{k,k+1} \tag{8}$$

The modified algorithm is conceptually represented by Eq. (8), identical to Eq. (4) except that sub-iterations on Δq^k are accommodated and a constant time step is used. Equation (6) is modified in a similar manner. The superscript (k, k+1) signifies that the latest available iterate on $\bar{q}^n + \Delta q^k$ is utilized in the evaluation of $\bar{r}_L$. Also, $\bar{r}_L$ now includes the time derivative term $(q_L^{n+1} - q_L^n)\Omega_L / \Delta t$. In theory, Eq. (8) is iterated on all cells until $\Delta\bar{q}^{k+1} = q^{k+1} - q^k$ is converged to order Δt^2 for first-order temporal accuracy. In practice $\bar{q}^{n+1}$ is updated after 10 to 20 sub-iterations on index k before advancing to time step n+2.

3 APPLICATIONS

Two configurations are discussed in which a steady state (or near steady state) could only be computed by executing a time accurate simulation. The steady state solution is believed to be correct for the ideal boundary conditions applied here in which all boundary conditions are steady and the incoming flow is uniform. Possibly, these geometries are also more sensitive to flow non-uniformities that trigger unsteady response in ground-based or flight experiments.

3.1 Concave Ballute

Large, inflatable ballutes (balloon-parachutes) have been proposed[11,12] as hypersonic decelerators for planetary aerocapture applications. Simulations of candidate configurations (spheres, toroids) for towed decelerators have been presented previously. Parachute-like configurations were also simulated in the early phases of the study but were abandoned because of concerns regarding flow stability and aerodynamic stability. The chute configurations failed to converge using the constant Courant number relaxation scheme. Rather, they showed a periodic growth and collapse of the shock wave, the extremes of which are shown in Figure 1 for a simple Mach 6, perfect gas flow. Instabilities have been reported previously in blunt body flows with cavities[5]. While the magnitude of these chute instabilities was larger than previously reported for the blunt body with cavity, their occurrence did not seem unreasonable at the time.

Additional variations of the relaxation scheme have been tested on this case – all starting from the same initial condition. The observations that follow were taken from movies in which a new frame is shown every 10^{th} time step. The solution was relaxed using the baseline, local-time stepping, point-implicit algorithm with Courant numbers of 10^0, 10^1, and 10^6. All cases showed unsteady, periodic motion. The amplitude of the shock motion was largest for the largest Courant number.

This test was repeated using the constant time step but varying the number of sub-iterations over values of 1, 10, and 20. Larger number of sub-iterations promotes improved time accuracy. Point-implicit relaxation is used unless otherwise noted. The unsteady response is still very strong with only one sub-iteration (baseline algorithm except with constant time step rather than constant Courant number.) The test with ten sub-iterations exhibited small but persistent oscillations that never damped over 25 cycles. The periodic response with constant amplitude was observed after 12 cycles. The test case with 20 sub-iterations achieved a near steady state (shock stand-off varied less than 1% after approximately 8 cycles.) Repeating this case with line-relaxation from the same initial condition led to a steady state in fewer relaxation steps. Line relaxation provides a greater level of convergence within the sub-iterations – consequently the temporal error, while still only first-order accurate, is reduced.

The effect of sub-iterations on the convergence of a constant Courant number simulation was studied. Twenty sub-iterations were executed on a case in which the Courant number was fixed at 10^1. This simulation also failed to achieve a steady state.

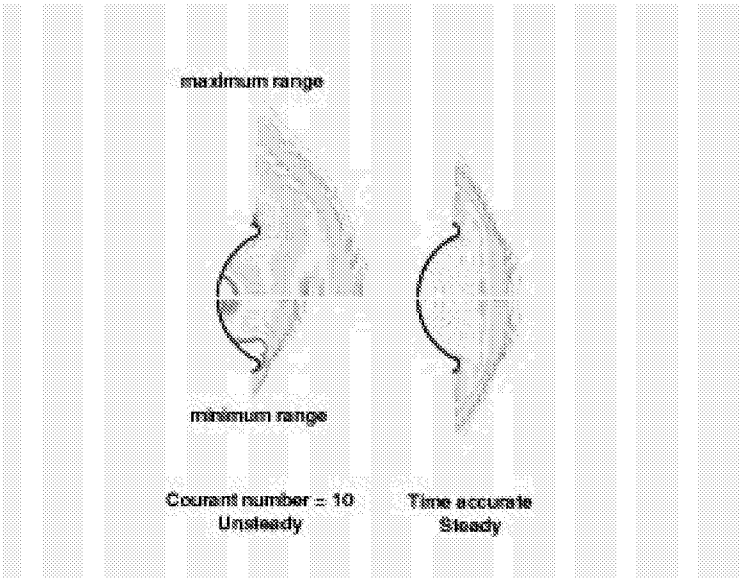

Figure 1: Density contours over chute at Mach 6 showing unsteady range of motion using constant Courant number simulation and steady solution from time-accurate simulation.

The LAURA code defaults to use of an alternating directional sweep through the domain from the body to the inflow boundary and back. Changing the sweep direction (axis to outflow and back) did nothing in the constant Courant number tests to promote convergence to a steady state.

In summary, the test problem requires a time accurate simulation to evolve to a steady state. Relaxation using a constant time step but insufficient sub-iterations to attain first-order time accuracy fails to produce a steady state. Multiple sub-iterations without the use of constant time steps fail to converge as well.

3.2 Sharp, Double-Cone

This unexpected result in which the ability to achieve a steady state requires temporal accuracy has not been observed previously in typical, convex blunt body geometries. However, in a recent hypersonic code validation study[1], simulated flow over a sharp, double cone (25^o / 55^o) at Mach 9.5 and Reynolds number 264000 m^{-1} in nitrogen showed large scale, periodic shedding of vortices in the separation region around the 30^o compression. A 1^{st} order accurate (in space), constant Courant number, simulation showed a steady flow for this same case. A 2^{nd} order simulation at a lower Reynolds number (144000 m^{-1}) showed a steady flow result on the same grid. Experimental data[2] in the Calspan – University at Buffalo Research Center (CUBRC) Large Energy National Shock (LENS) tunnel for this case (Run 24) from thin-film heat transfer gauges indicated that the flow achieved steady state in the test time. The non-linear minmod flux limiter[3] in LAURA was a suspected source of numerical ringing within the recirculation region that triggered the unsteadiness.

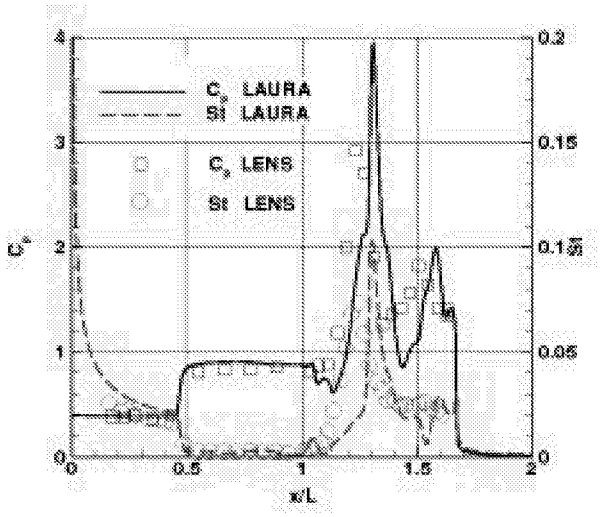

Figure 2: Pressure and heating over sharp, double cone for Run 24 of Reference 2 using time-accurate simulation to attain steady state.

In light of these recent results showing that attainment of a steady state can depend on temporal accuracy in some circumstances, the sharp, double- cone case was revisited using time-accurate simulation. The time step was set at 3.65 10^{-7} s. The reference flow time, L / V_∞, is 7.08 10^{-5} s. The flow converged to a nearly steady state – very slight oscillation of streamlines persisted in the recirculation region, but these oscillations were orders of magnitude less severe than observed in the constant Courant number simulation. Comparisons with experimental data for pressure and heating are presented in Figure 2. Good agreement with the onset of separation is observed. Fair agreement with reflected wave peak pressure and heating location is obtained. The broad, flat

pressure plateau in the recirculation region for $0.5<x/L<1$ had significant, varying structure in the previous, constant Courant number simulation.

Both the chute and double-cone cases have a subsonic region contained in a concavity (rays perpendicular to the surface converge in a subsonic domain) driven by an external supersonic flow. In the typical grid that is highly stretched from the body a constant Courant number simulation means that physical time advances more rapidly away from the body than in close to the body. A similar argument is suggested for cases in which a constant time step is used but temporal errors are largest in the near wall region if an insufficient number of sub-iterations are applied. Perturbations associated with each relaxation step may tend to aggregate near the wall in the concavity before exiting a supersonic outflow boundary. Waves accumulate (in this non-physical temporal map), strengthen, and reflect back in to the subsonic domain in a self-sustaining but non-physical manner. This scenario is consistent with observed behavior in the two systems tested here. Certainly, not all subsonic domains with concavities induce this pseudo-unsteady behavior in constant Courant number simulations – there are many examples of compression corners with separated flow being computed with constant Courant number relaxation. It is simply noted that such flow conditions may be susceptible to pseudo-unsteady behavior in non-time-accurate relaxation and the overhead associated with implicit, time-accurate simulation may be recovered with better convergence.

4 CONCLUDING REMARKS

Point- and line-implicit relaxation algorithms within Program LAURA are reviewed. Modifications involving sub-iterations to achieve temporal accuracy are defined for the purpose of investigating their effect on convergence. Hypersonic flows with subsonic regions bounded by a local concavity are observed to support periodic, unsteady behavior using a constant Courant number relaxation but recover a steady flow behavior using time-accurate simulation. The test problems require a time-accurate simulation to evolve to a steady state. Relaxation using a constant time step but insufficient sub-iterations to attain first-order time accuracy fails to produce a steady state. Multiple sub-iterations without the use of constant time steps fail to converge as well. The behavior is thought to emerge from the temporal mapping of local time stepping allowing accumulated perturbations to reflect back into the subsonic domain.

5 REFERENCES

[1] Gnoffo, P. A.: "CFD Validation Studies for Hypersonic Flow Prediction," AIAA 2001-1025, Jan. (2001).

[2] Holden, M. S. and Wadhams, T. P.: "Code Validation Study of Laminar Shock/Boundary Layer and Shock/Shock Interactions in Hypersonic Flow Part A: Experimental Measurements," AIAA 2001-1031, Jan.(2001).

[3] Yee, H. C.: "Upwind and Symmetric Shock-Capturing Schemes," NASA TM 89464, May (1987).

[4] Gnoffo, Peter A.: "Computational Aerothermodynamics in Aeroassist Application," AIAA 2001-2632, June (2001).

[5] Huebner, L. D. and Utreja, L. R.: "Mach 10 Bow-Shock Behavior of a Forward-Facing Nose Cavity," JSR, Vol. 30, No. 3, pp291-297, May-June (1993).

[6] Gnoffo, P. A.; Gupta, R. N.; and Shinn, J.: "Conservation Equations and Physical Models for Hypersonic Air Flows in Thermal and Chemical Nonequilibrium," NASA TP 2867, (1989).

[7] Cheatwood, F. M. and Gnoffo, P. A.: "User's Manual for the Langley Aerothermodynamic Upwind Relaxation Algorithm (LAURA)", NASA TM 4674, April (1996).

[8] Roe, P. L.: "Approximate Riemann Solvers, Parameter Vectors, and Difference Schemes",*J. Comput. Phys.,* vol. 43, no. 2, pp. 357-372, Oct. (1981).
[9] Harten, Ami: "High Resolution Schemes for Hypersonic Conservation Laws", *J. Comput. Phys.,* vol. 49, no. 2, pp. 357-393, Feb. (1983).
[10] Mitterer, K. F.; Mitcheltree, R. A.; and Gnoffo, P. A.: "Application of Program LAURA to Perfect Gas Shock Tube Flows – A Parametric Study", NASA TM 104190, January (1992).
[11] Hall, J. L.: "A Review of Ballute Technology for Planetary Aerocapture", Presented at the 4th IAA Conference on Low Cost Planetary Missions, Laurel, MD, May (2000).
[12] Hall, Jeffery L.; and Le, Andrew K.: "Aerocapture Trajectories for Spacecraft with Large Towed Ballutes," Paper AAS 01-235, Feb (2001).